Electronic Supporting Information for:

Drug delivery and controlled release on biocompatible metal-organic frameworks using mechanical amorphization

Claudia Orellana-Tavra,[a] Ross J. Marshall,[b] Emma F. Baxter,[c] Isabel Abanades Lazaro,[b] Andi Tao,[a] Anthony K. Cheetham,[c] Ross S. Forgan[b,] and David Fairen-Jimenez[a,*]*

[a]Adsorption & Advanced Materials Laboratory (AAML), Department of Chemical Engineering & Biotechnology, University of Cambridge, Pembroke Street, Cambridge CB2 3RA, UK. Email: df334@cam.ac.uk; website: http://people.ds.cam.ac.uk/df334

[b]WestCHEM School of Chemistry, University of Glasgow, Joseph Black Building, University Avenue, Glasgow, G12 8QQ, UK. Email: ross.forgan@glasgow.ac.uk; website: http://www.forganlab.com

[c]Department of Materials Science and Metallurgy, University of Cambridge, CB3 0FS Cambridge, UK

Contents

S1. Powder X-Ray Diffraction (PXRD)

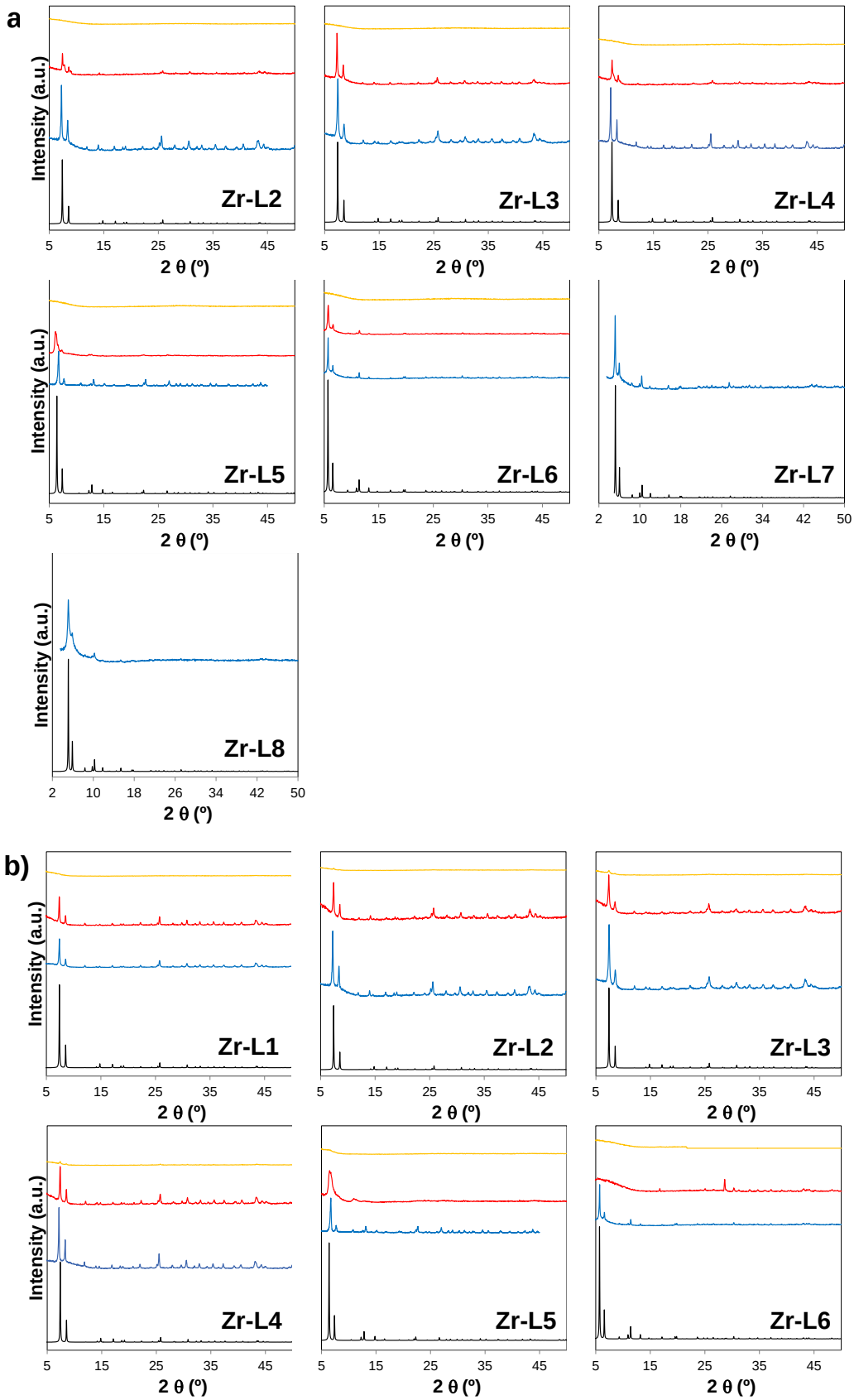

Figure S1. Powder X-ray diffraction (PXRD) patterns of synthesized Zr-based MOFs compared with the calculated pattern for each. Colour code of patterns: black, calculated; blue, synthesized; red, loaded; and, yellow, amorphisized. a) calcein loaded materials and, b) α-CHC loaded materials.

S2. Scanning electron microscopy (SEM)

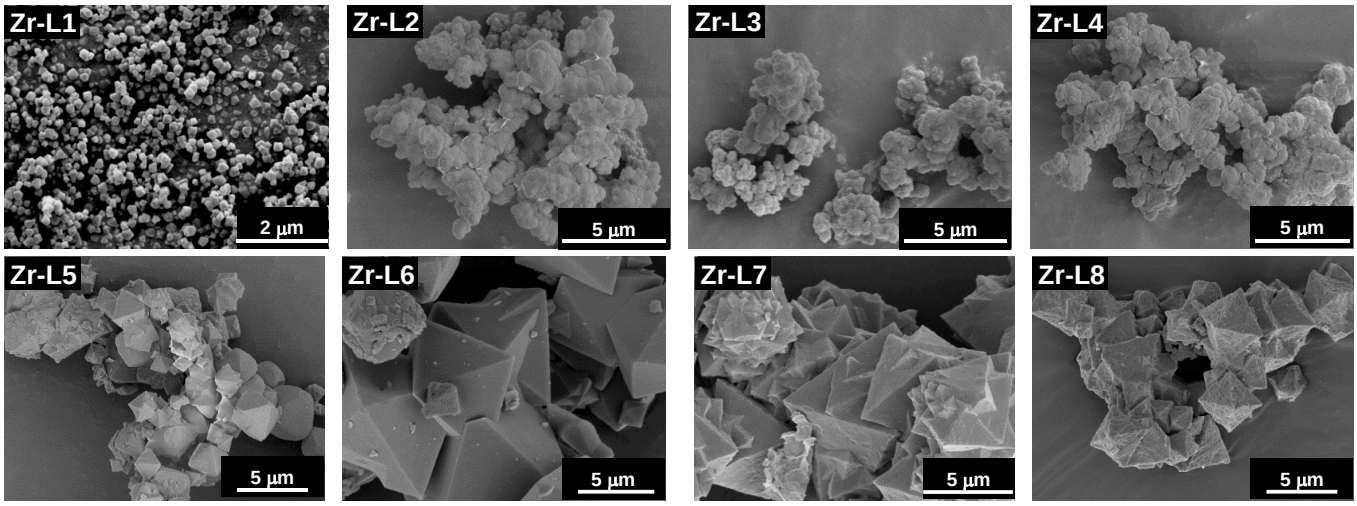

Figure S2. SEM images for Zr-based MOFs, Zr-L1 to Zr-L8.

S3. Nitrogen adsorption isotherms: experimental and simulated

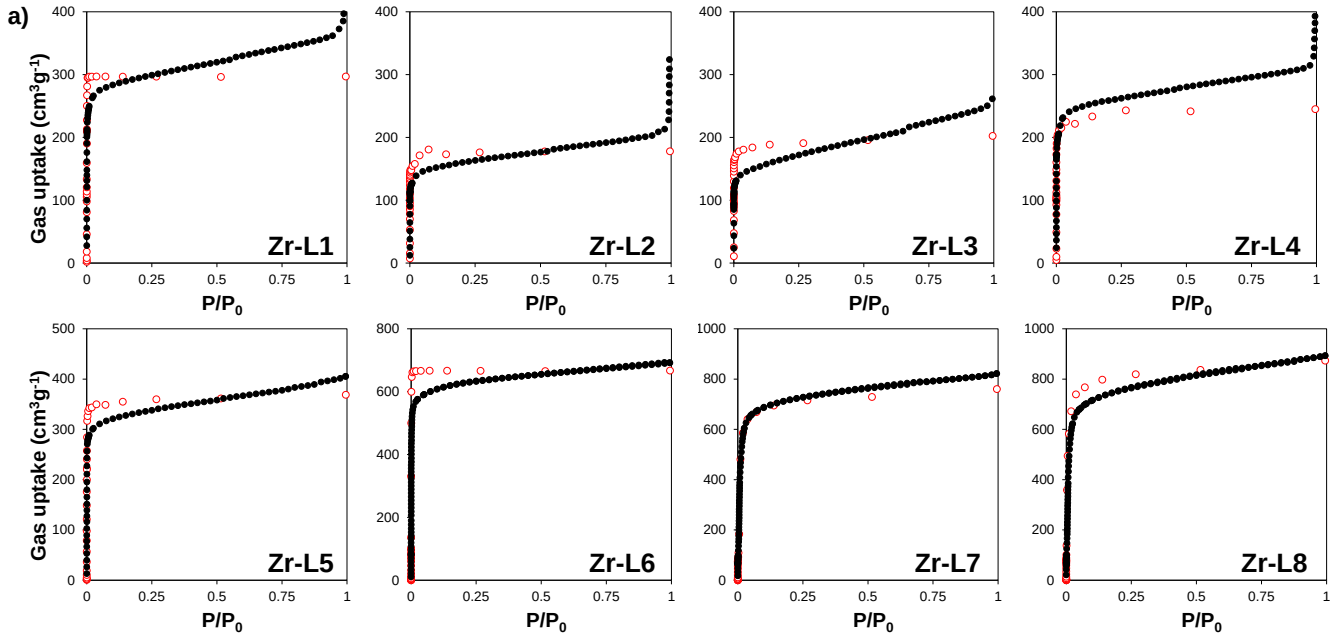

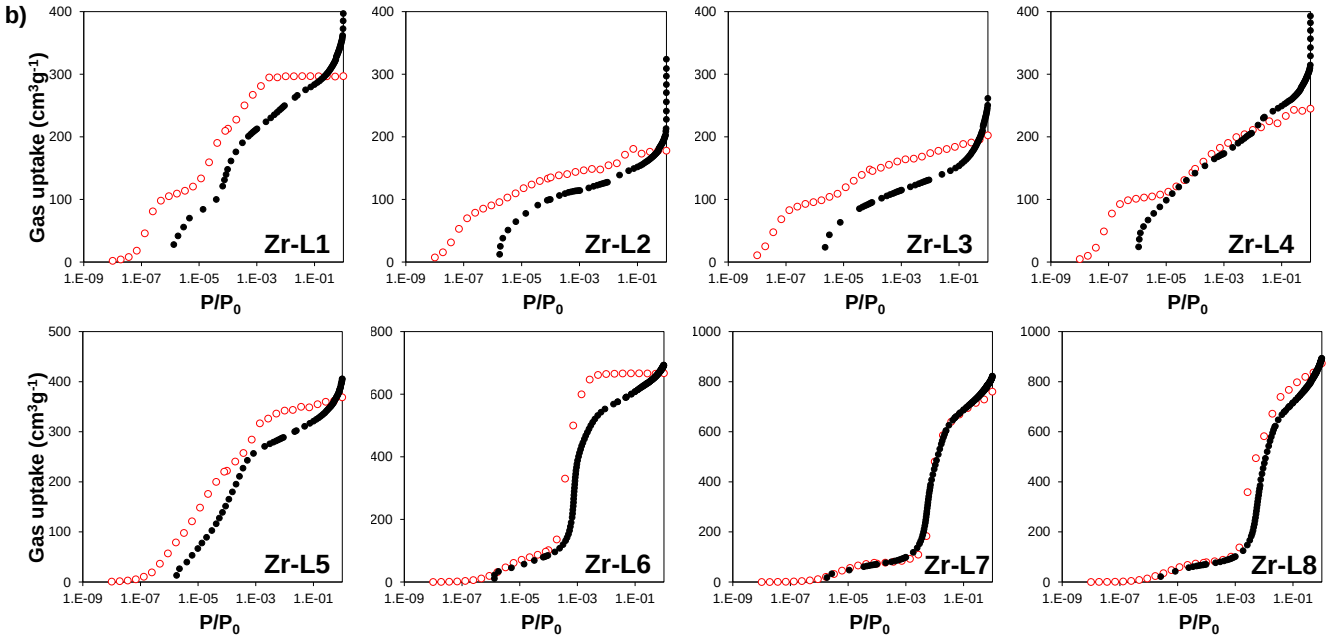

Figure S3. N_2 adsorption isotherms for Zr-based family, experimental (black closed dots) and simulated (red opened dots). a) linear scale; b) semi-log scale.

S4. Pore size distribution analysis (PSD)

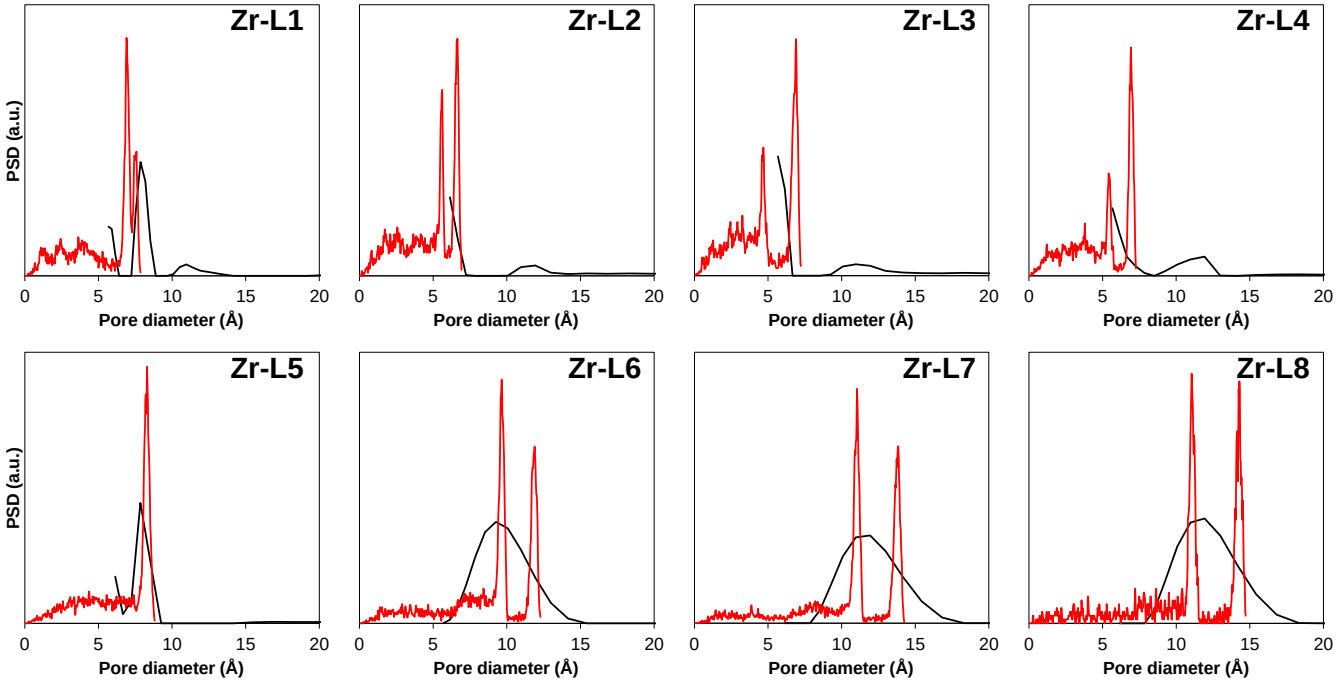

Figure S4. PSD analysis for Zr-based family, experimental (black continued line) and simulated (red continued line).

S5. Stability analysis

The kinetics of degradation from the solids were adjusted using non-linear regressions in order to understand their behaviour. For Zr-L1 to Zr-L8 in PBS, and Zr-L2 to Zr-L7 in H_2O the profile was adjusted to a simple hyperbola model [1]:

$$\text{N (wt. \%)} = \frac{N_{max}\, t}{(t_{1/2} + t)} \quad [1]$$

where N is the amount of linker released from the solid, Nmax is the maximum amount released, t is time in days and $t_{1/2}$ is the time needed to get half of the maximum amount delivered.

For Zr-L1 in H2O it was not possible to adjust the delivery to a simple curve. Instead, we used a hyperbola model considering two different release stages [2]:

$$\text{N (wt. \%)} = \frac{N_{\max}(1)\, t}{(t_{1/2}(1) + t)} + N_2\, t + a \quad [2]$$

where Nmax and $t_{1/2}$ are considered for the first stage of delivery and N2 and a are the slope and intercept of the linear part of the release.

For Zr-L8 in H2O, we used a hyperbola model considering a slope factor or Hill slope, which is related with the interactions material-solvent [3]:

$$\text{N (wt. \%)} = \frac{N_{\max} t\text{^h}}{(t_{1/2}\text{^h} + t\text{^h})} \quad [3]$$

where Nmax is the maximum amount released, t is time in days and $t_{1/2}$ is the time needed to get half of the maximum amount delivered and h is the Hill slope.

Figure S4 and Tables S1 show the fitting of the degradation in PBS and H2O of the materials.

Table S1: Fit-curves for degradation profiles of Zr-based MOFs.

	PBS		H_2O	
MOF	**Equation**	**R^2**	**Equation**	**R^2**
Zr-L1	linker (wt%) = 76.33 t / (0.004959 + t)	0.9943	linker (wt%) = 34.61 t / (0.04002 + t) + 1.111*t - 0.6783	0.9641
Zr-L2	linker (wt%) = 76.23 t / (0.003767 + t)	0.9962	linker (wt%) = 5.170 t / (4.693 + t)	0.9963
Zr-L3	linker (wt%) = 90.75 t / (0.003325 + t)	0.9945	linker (wt%) = 8.753 t / (3.610 + t)	0.9877
Zr-L4	linker (wt%) = 57.92 t / (0.01034 + t)	0.9936	linker (wt%) = 0.1868 t / (0.08060 + t)	0.9238
Zr-L5	linker (wt%) = 69.66 t / (0.04697 + t)	0.9640	linker (wt%) = 0.3950 t -0.01018	0.9943
Zr-L6	linker (wt%) = 100.4 t / (0.09548 + t)	0.9980	linker (wt%) = 3.603 t / (3.867 + t)	0.9949
Zr-L7	linker (wt%) = 95.06 t / (0.07875 + t)	0.9897	linker (wt%) = 98.08 t / (4.097 + t)	0.9887
Zr-L8	linker (wt%) = 90.59 t / (0.07071 + t)	0.9847	linker (wt%) = 14.77 t^7.286 / (1.621^7.286 + t^7.286)	0.9965

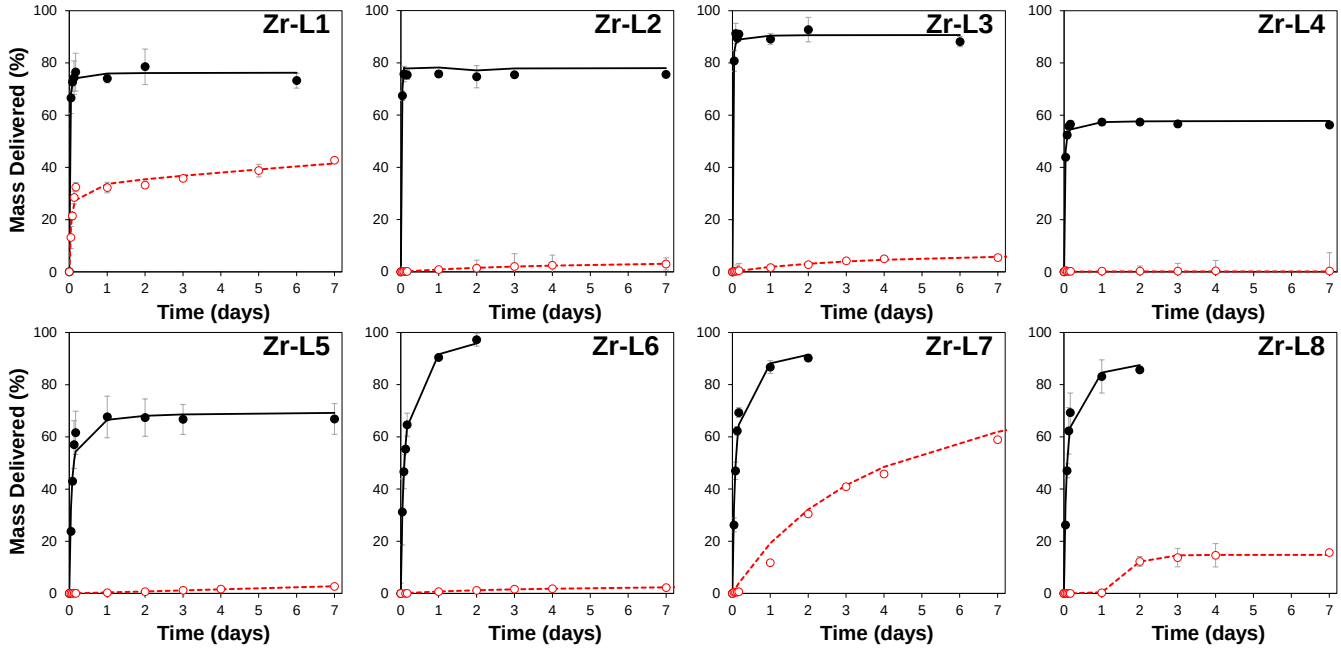

Figure S5. Stability analysis of Zr-based MOFs in PBS (black closed dots) and H_2O (red opened dots).

S6. XRD analysis after PBS exposure

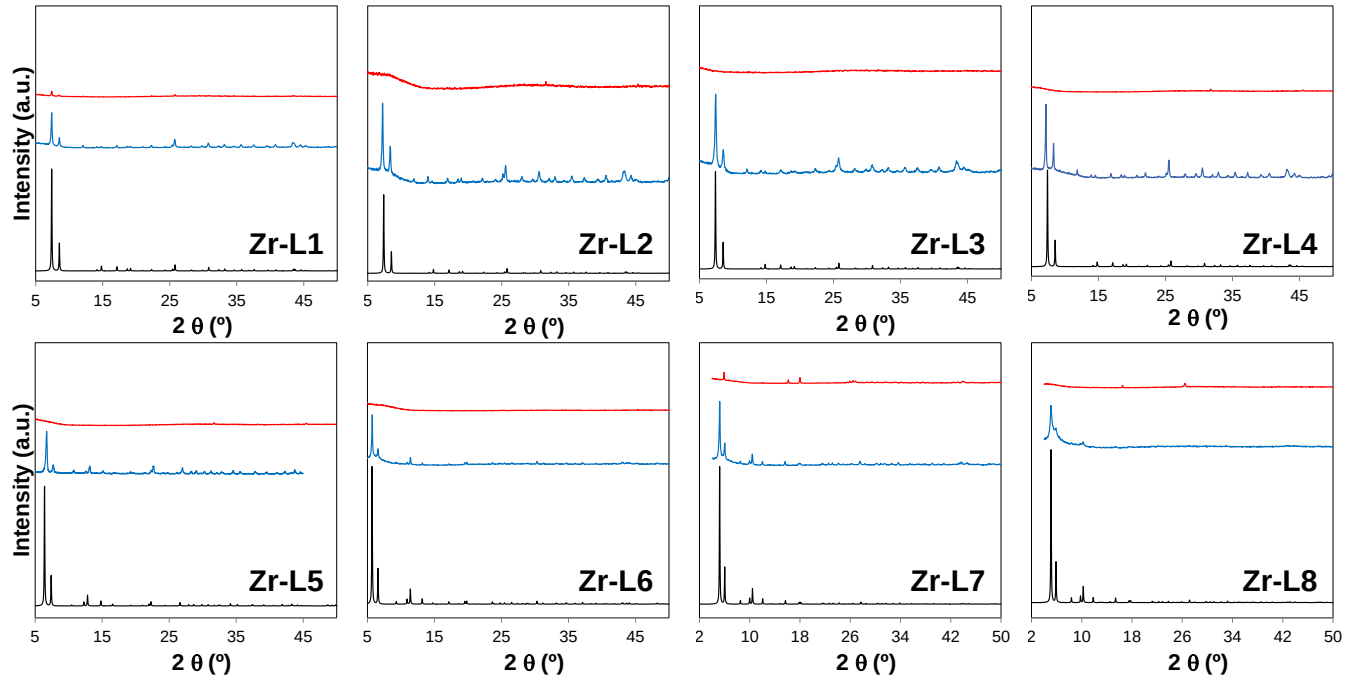

Figure S6. PXRD analysis of Zr-based MOFs after PBS exposure for 2 days. Color code of patterns: black, calculated; blue, synthesized; red, degraded after 2 days in PBS.

S7. FTIR

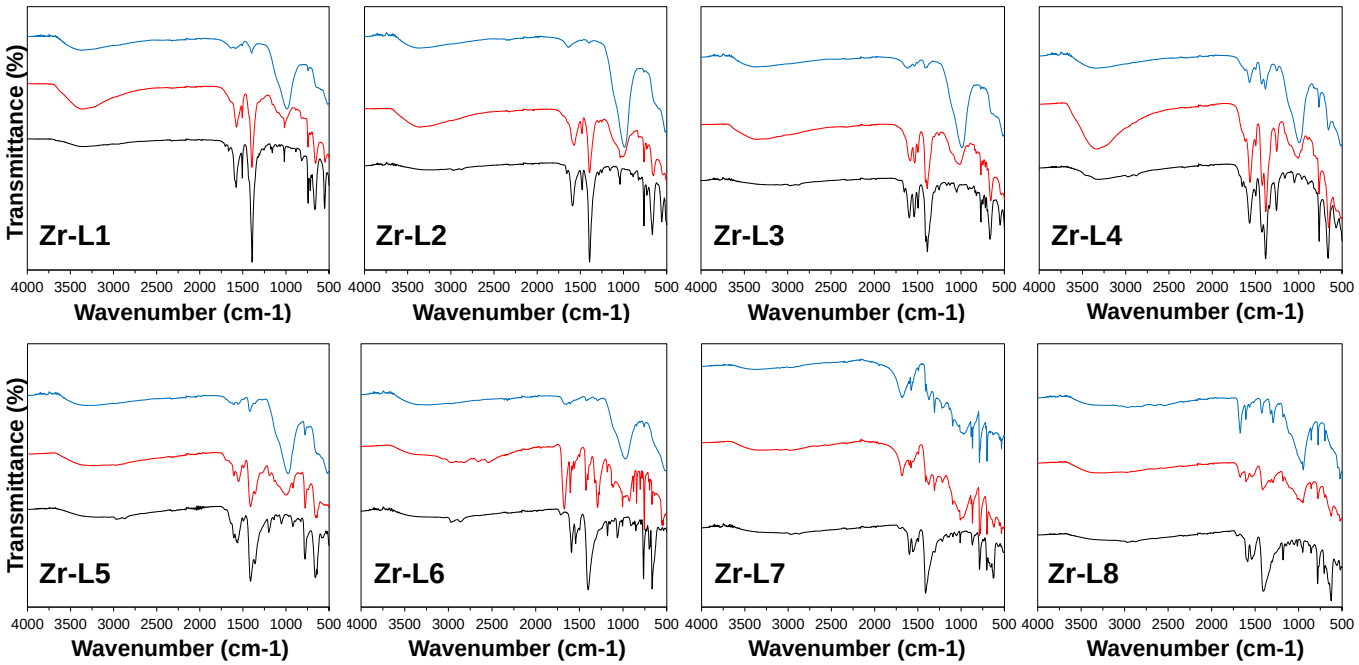

Figure S7. FTIR analysis of Zr-based MOFs after PBS exposure. Color code of patterns: black, no exposure to PBS; red, 2 days; and, blue, 3 days of PBS exposure.

S8. Cytotoxicity analysis

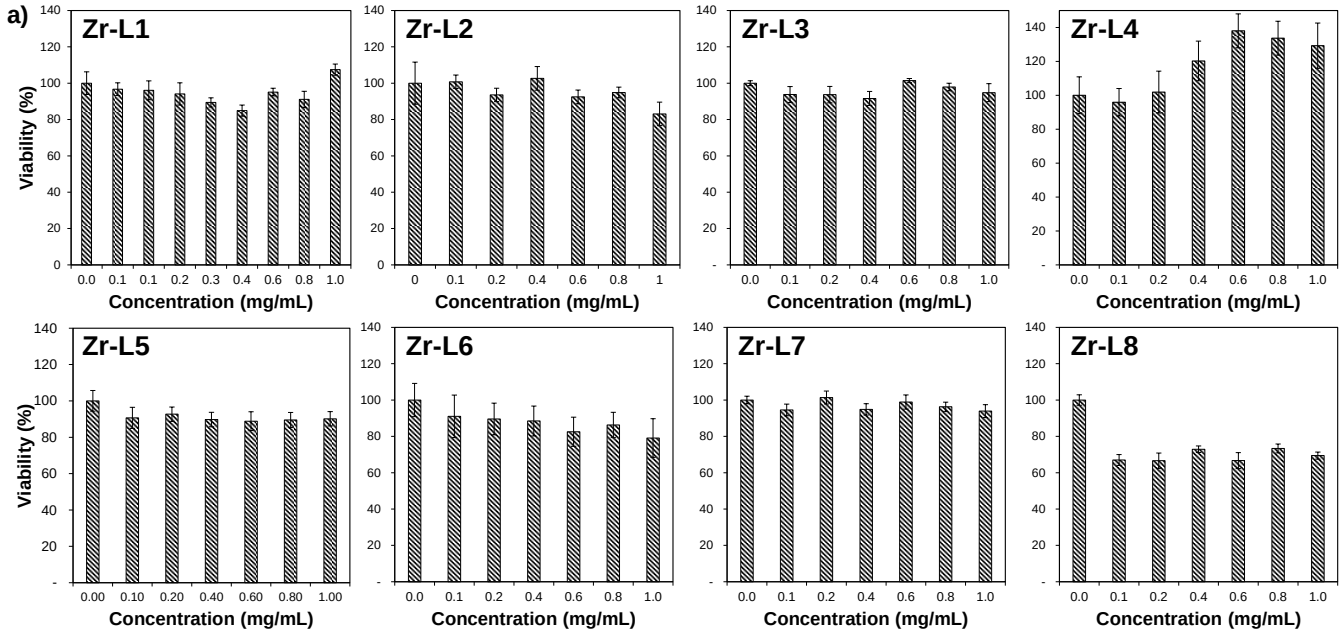

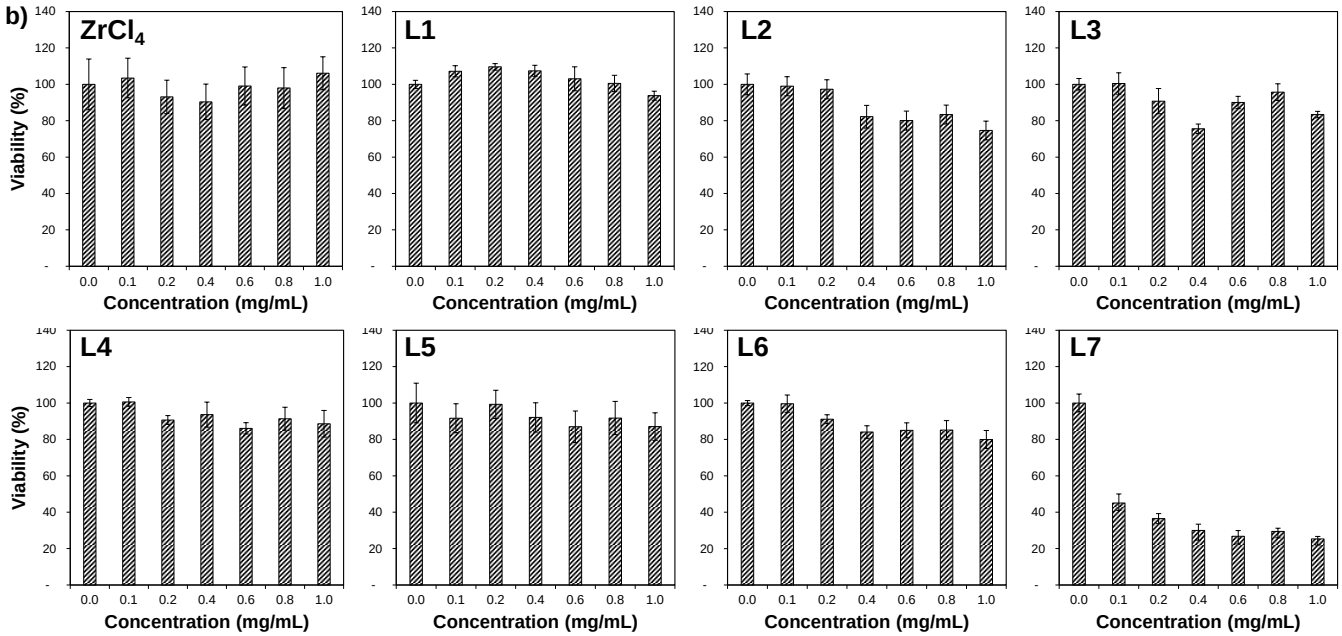

Figure S8. Cytotoxicity analysis. a) MTS assay for Zr-based MOFs; b) MTS assay for zirconium tetrachloride and each organic linker of the Zr-based family. L8 was not measured as Zr-L8 showed cytotoxicity.

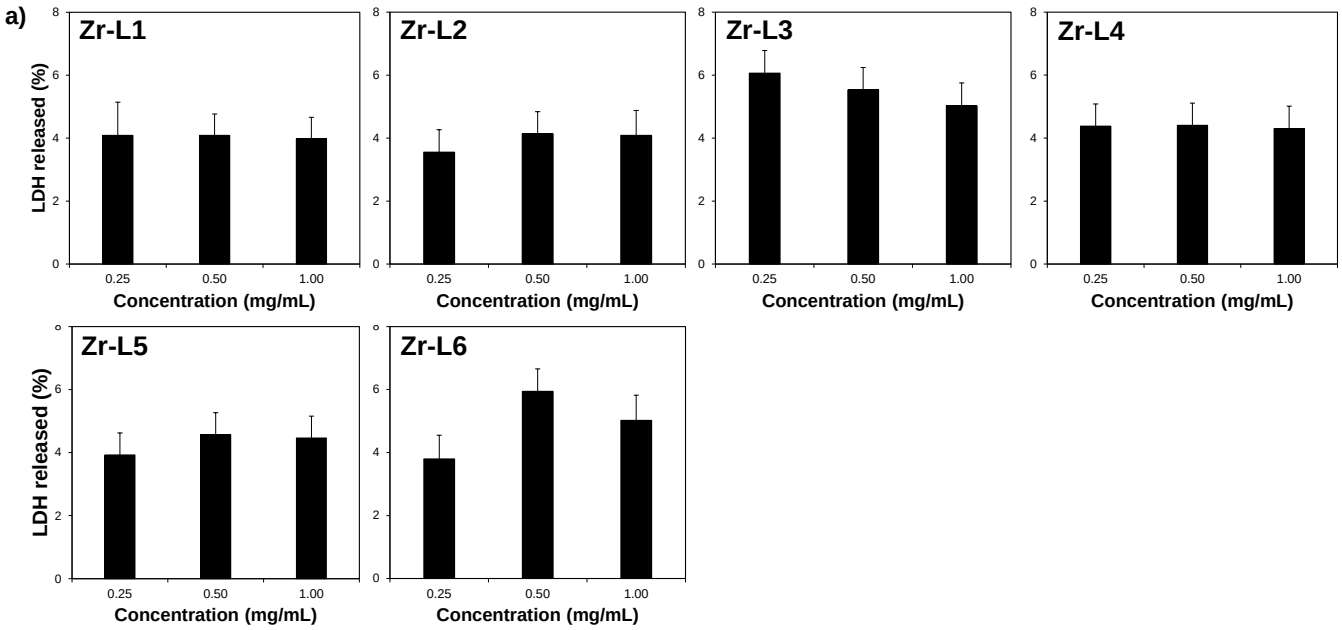

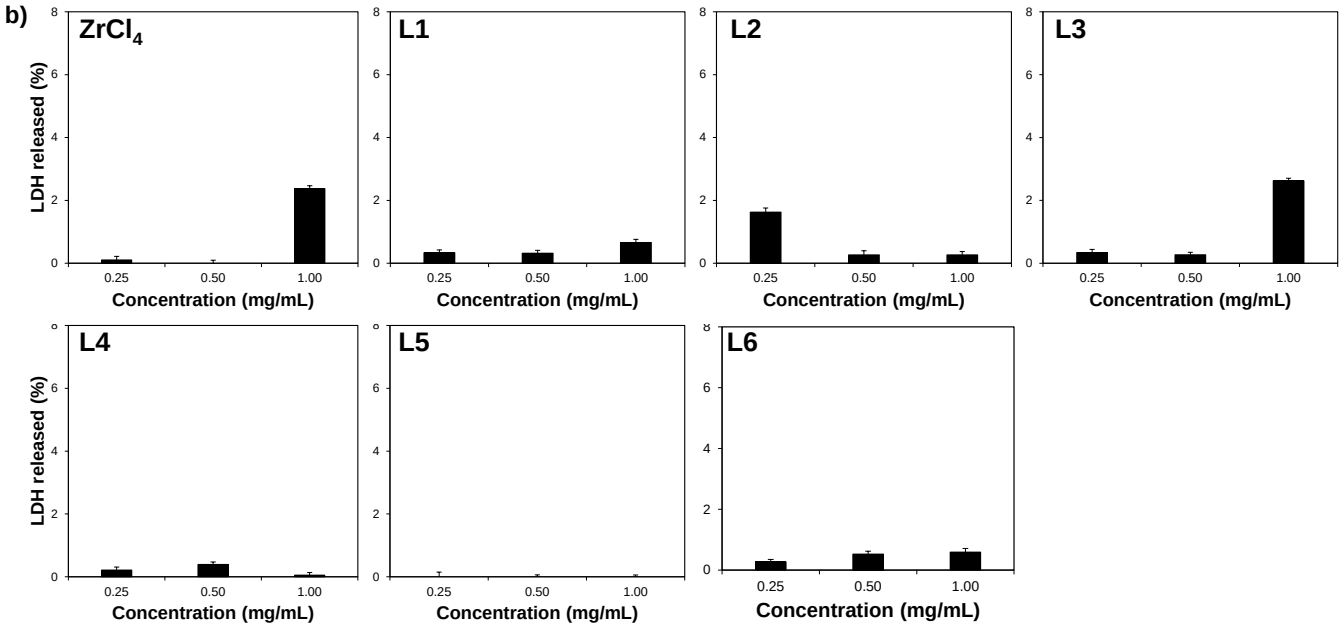

Figure S9. Cytotoxicity analysis. a) LDH assay for Zr-based MOFs and b) LDH assay for zirconium tetrachloride and each organic linker of the Zr-based MOF family.

S9. Thermogravimetric analysis (TGA)

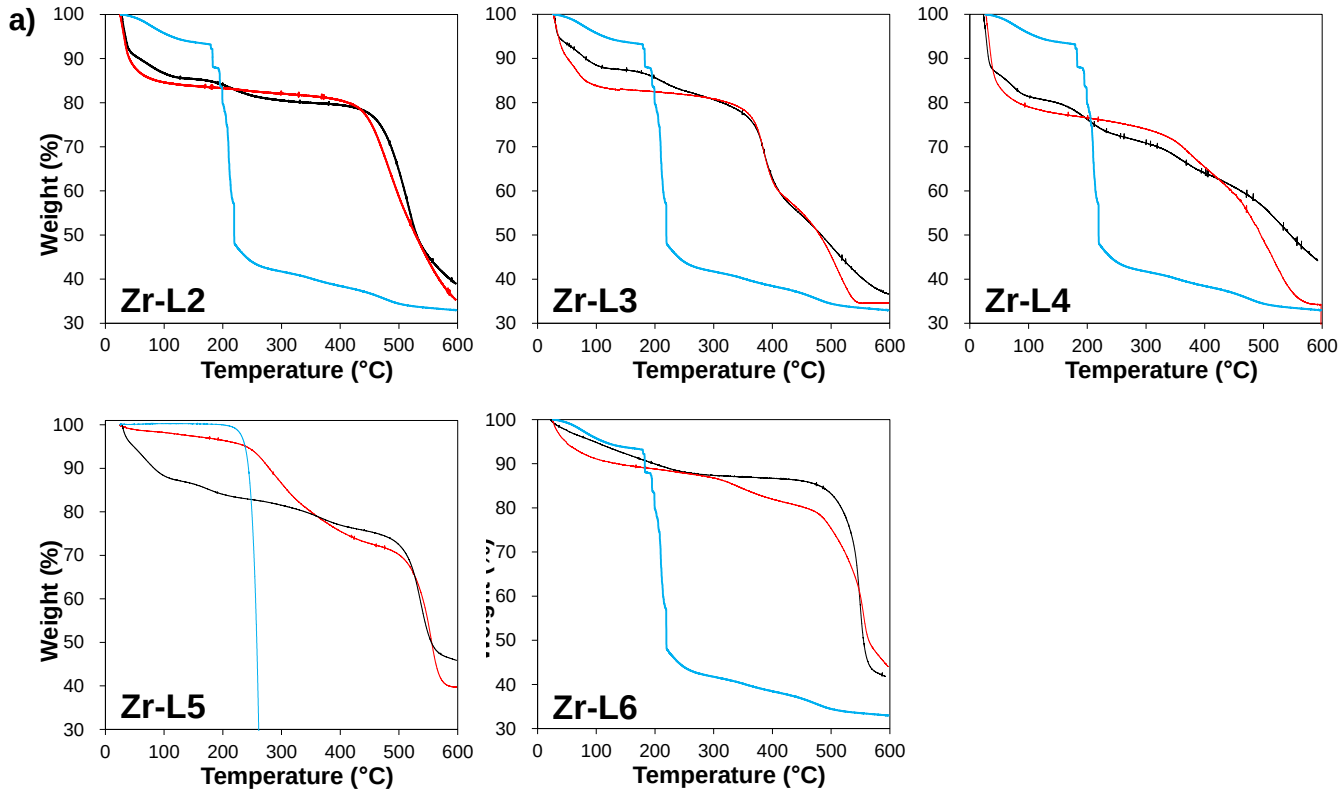

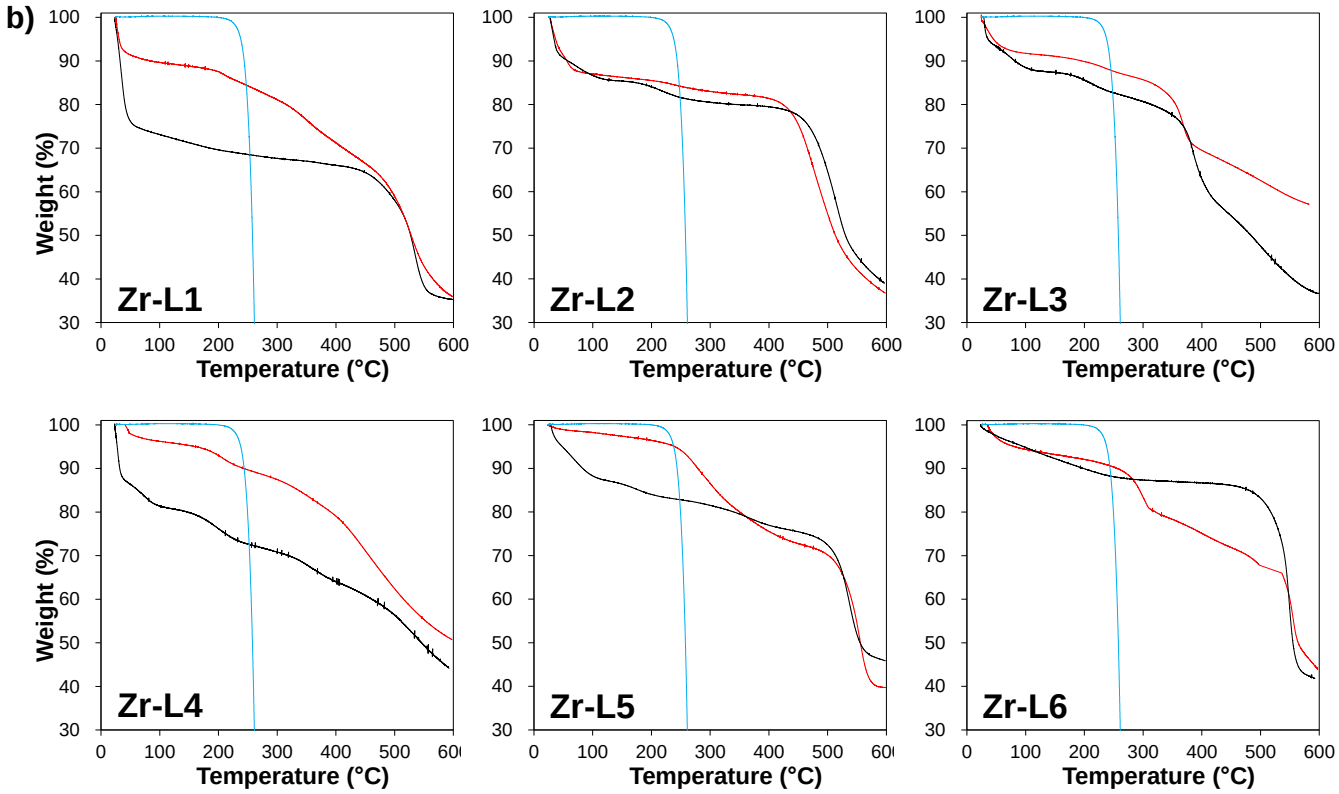

Figure S10. Thermogravimetric analysis (TGA) of synthesized Zr-based MOFs compared with the loaded material. a) calcein loaded materials and, b) α-CHC loaded materials. Color code of patterns: black, empty material; red, loaded material; blue, free drug.

S10. Delivery profiles from crystalline and amorphous Zr-based family

The kinetics of calcein and α-CHC delivery from crystalline and amorphous solids were adjusted using non-linear regressions in order to understand the release behaviour. For the calcein loaded Zr-L3 to Zr-L6, a$_m$Zr-L3 and a$_m$Zr-L6 materials the delivery was adjusted to a simple hyperbola model [4]:

$$\text{N (wt. \%)} = \frac{N_{max}\, t}{(t_{1/2} + t)} \qquad [4]$$

where *N* is the amount released from the total drug-loaded amount in weight percent, *Nmax* is the maximum amount released, *t* is time in days and $t_{1/2}$ is the time needed to get half of the maximum amount delivered.

For the calcein loaded Zr-L2, a$_m$Zr-L2, a$_m$Zr-L4, a$_m$Zr-L5 and all the α-CHC loaded materials (crystalline and amorphous) it was not possible to adjust the delivery to a simple curve. Instead, we used a hyperbola model considering two different release stages [5]:

$$\text{N (wt. \%)} = \frac{N_{\max}(1)\,\text{t}}{(t_{1/2}(1) + \text{t})} + \text{N}_2\, t + a \qquad [5]$$

where N_{max} and $t_{1/2}$ are considered for the first stage of delivery and N_2 and a are the slope and intercept of the linear part of the release.

Figure S8 and Tables S2 and S3 show the fitting of the experimental release and fitting parameters, respectively, for calcein loaded and α-CHC loaded materials. In both cases, as it was possible to detect the calcein and α-CHC delivered form all the amorphous materials it is possible to conclude that the ball-milling process is not provoking the release of guest molecules.

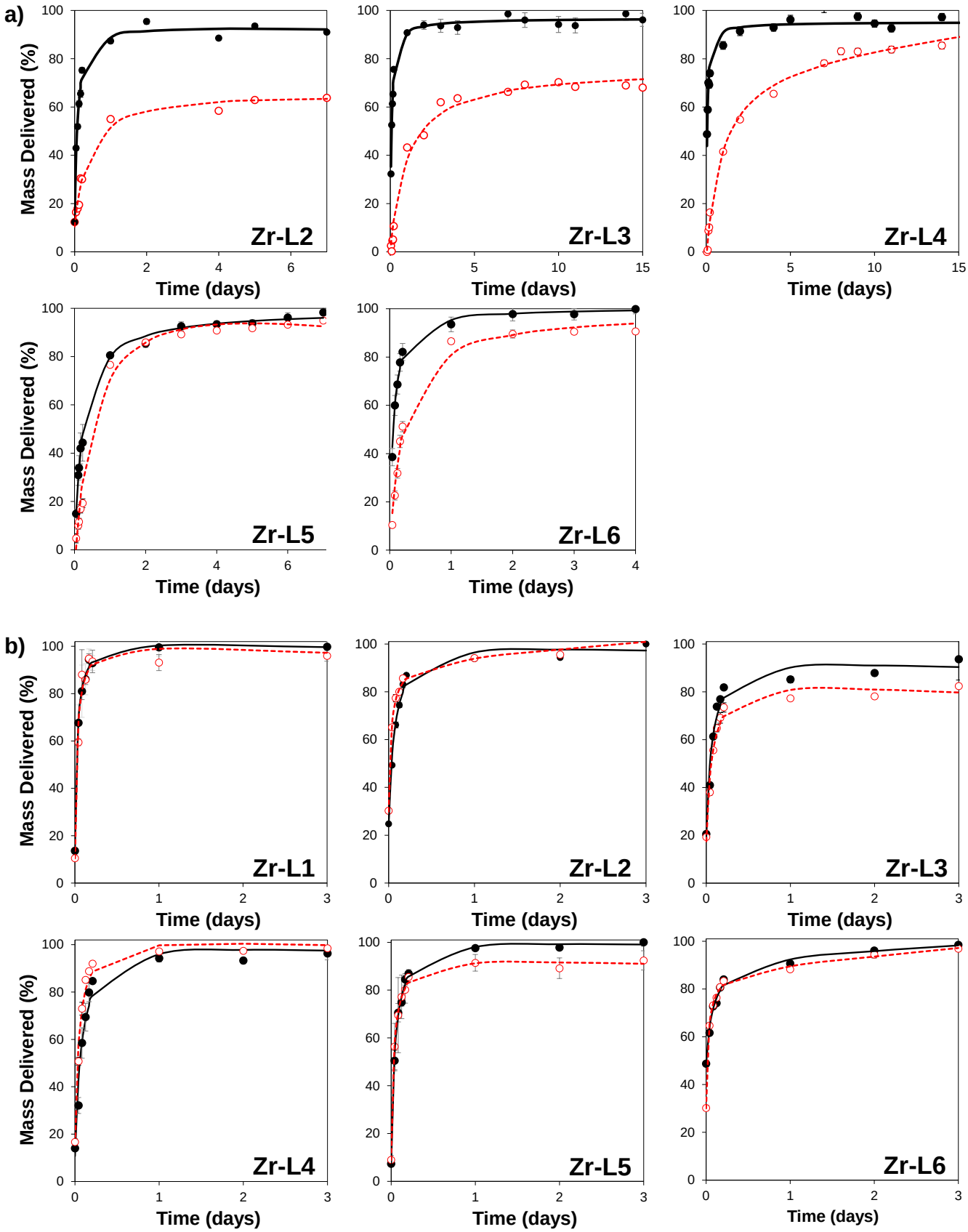

Figure S11. Release profile of a) calcein and b) α-CHC from the crystalline (in black closed dots) and amorphous (in red opened dots) materials. Black solid and red dotted lines represent the kinetic of delivery fitting using non-linear regression on crystalline and amorphous materials, respectively.

Table S2: Fit-curves for calcein release from crystalline and amorphous Zr-based solids.

	Crystalline		Amorphous	
MOF	**Equation**	**R^2**	**Equation**	**R^2**
Zr-L2	cal (wt%) = 82.21 t / (0.08366 + t) - 0.3220*t + 13.14	0.9900	cal (wt%) = 58.09 t / (0.4098 + t) – 0.2811*t + 10.47	0.9879
Zr-L3	cal (wt%) = 96.73 t / (0.07250 + t)	0.9902	cal (wt%) = 76.26 t / (1.007 + t)	0.9858
Zr-L4	cal (wt%) = 95.21 t / (0.04873 + t)	0.9540	cal (wt%) = 84.62 t / (0.9402 + t) + 0.8159*t - 2.879	0.9958
Zr-L5	cal (wt%) = 99.42 t / (0.2481 + t)	0.9964	cal (wt%) = 126.3 t / (0.5592 + t) - 2.3040*t - 8.367	0.9824
Zr-L6	cal (wt%) = 100.7 t / (0.05676 + t)	0.9912	cal (wt%) = 99.27 t / (0.2279 + t)	0.9864

Table S3: Fit-curves for α-CHC release from crystalline and amorphous Zr-based solids.

	Crystalline		Amorphous	
MOF	**Equation**	**R^2**	**Equation**	**R^2**
Zr-L1	α-CHC (wt%) = 89.79 t / (0.02686 + t) - 1.111*t + 13.99	0.9973	α-CHC (wt%) =94.42 t / (0.02567 + t) – 1.595*t + 10.41	0.9738
Zr-L2	α-CHC (wt%) = 78.86 t / (0.06801 + t) - 1.226*t + 23.84	0.9836	α-CHC (wt%) = 62.84 t / (0.02967 + t) + 2.931*t + 29.91	0.9961
Zr-L3	α-CHC (wt%) = 77.37 t / (0.06562 + t) - 1.446*t + 18.99	0.9700	α-CHC (wt%) = 69.61 t / (0.06692 + t) - 1.948*t + 17.47	0.9776
Zr-L4	α-CHC (wt%) = 93.47 t / (0.07793 + t) – 1.420*t + 10.68	0.9753	α-CHC (wt%) = 89.24 t / (0.04578 + t) – 1.254*t + 15.70	0.9858
Zr-L5	α-CHC (wt%) = 96.202 t / (0.04517 + t) - 0.8328*t + 6.8	0.9964	α-CHC (wt%) = 85.93 t / (0.03250 + t) - 0.9927*t + 8.976	0.9974
Zr-L6	α-CHC (wt%) = 45.48 t / (0.08153 + t) + 1.833*t + 48.48	0.9832	α-CHC (wt%) = 57.66 t / (0.02727 + t) + 3.330*t + 30.01	0.9974

S11. SEM nano-sized particles

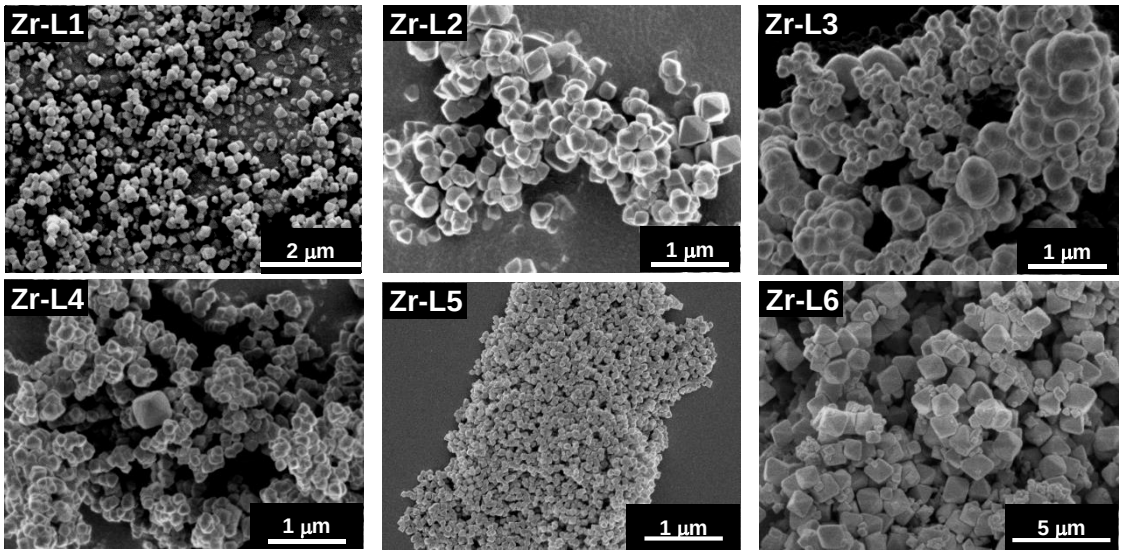

Figure S12. SEM images of nano-sized Zr-based MOFs.

S12. Cytotoxicity analysis of nano-sized particles

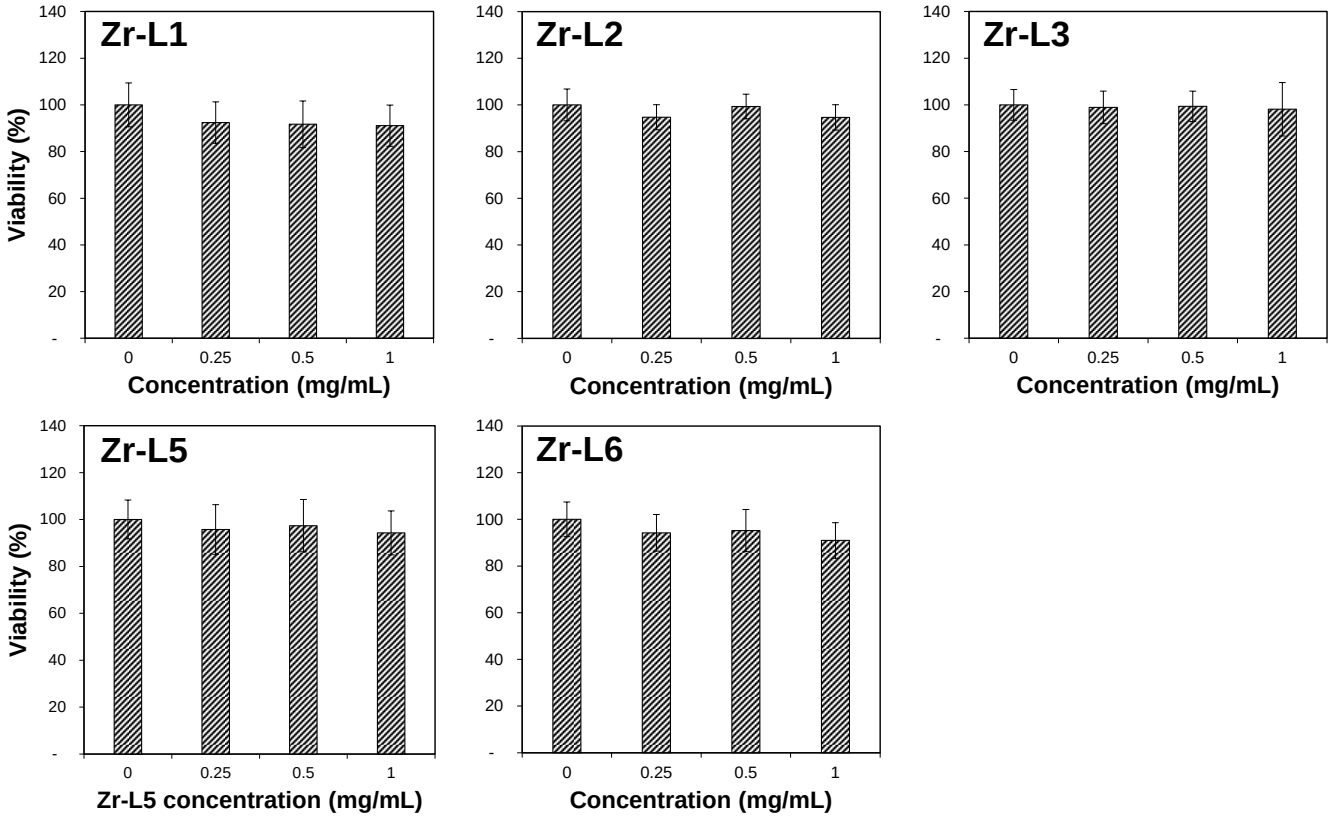

Figure S13. MTS assay of nano-sized Zr-based MOFs.

S13. Cytotoxicity analysis of α-CHC loaded nano-sized particles

Table S4: Loading values for α-CHC into Zr-based nano-sized materials. The values were measured using UV-vis. Loading value of Zr-L1 is the same presented before as this was the same exactly material.

MOF	α-CHC (wt.%)
Zr-L1	31
Zr-L2	1
Zr-L3	2
Zr-L4	4
Zr-L5	12
Zr-L6	20

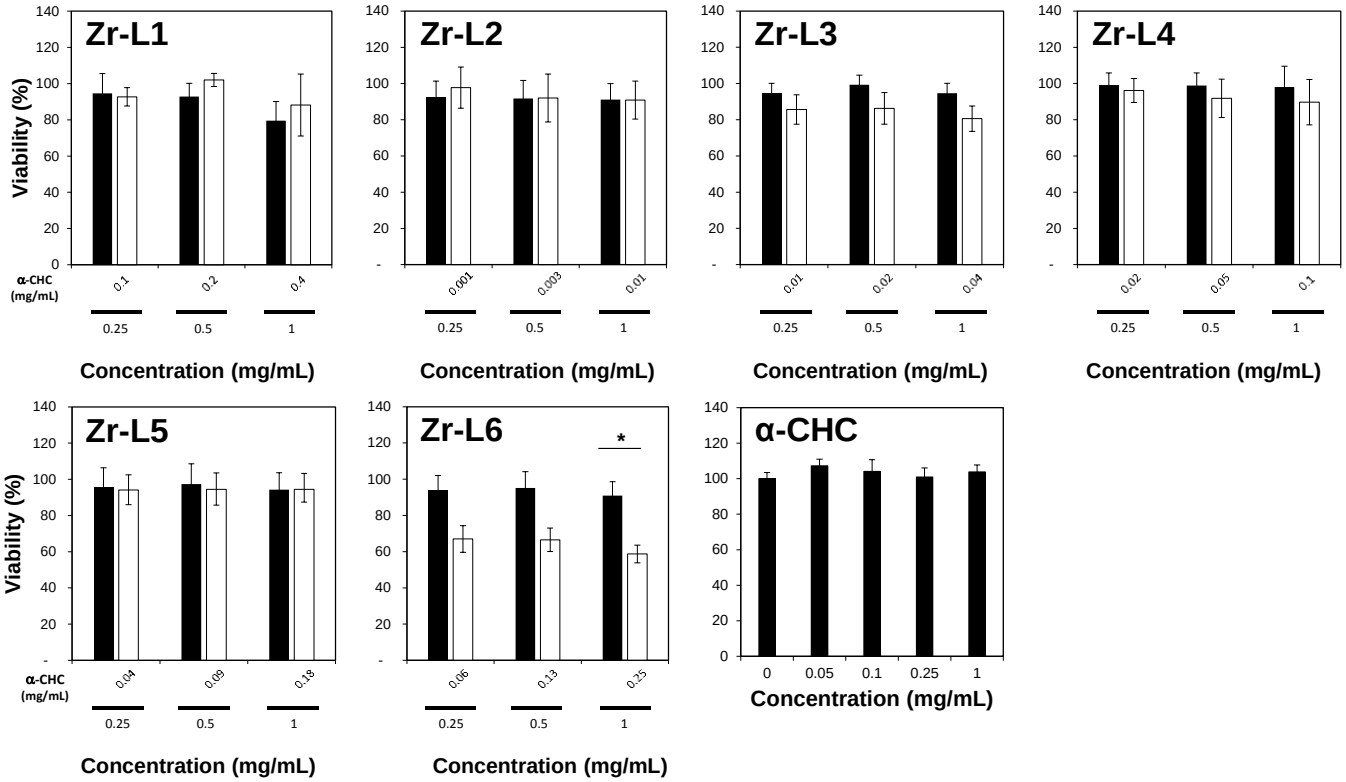

Figure S14. MTS assay of α-CHC loaded nano-sized Zr-based MOFs and free α-CHC. * indicates P ≤ 0.05 in comparison with the empty Zr-L6 MOF (Student's test). Black bars correspond to empty material and white ones to loaded MOF.

S14. Calibration curves of calcein and α-CHC in PBS

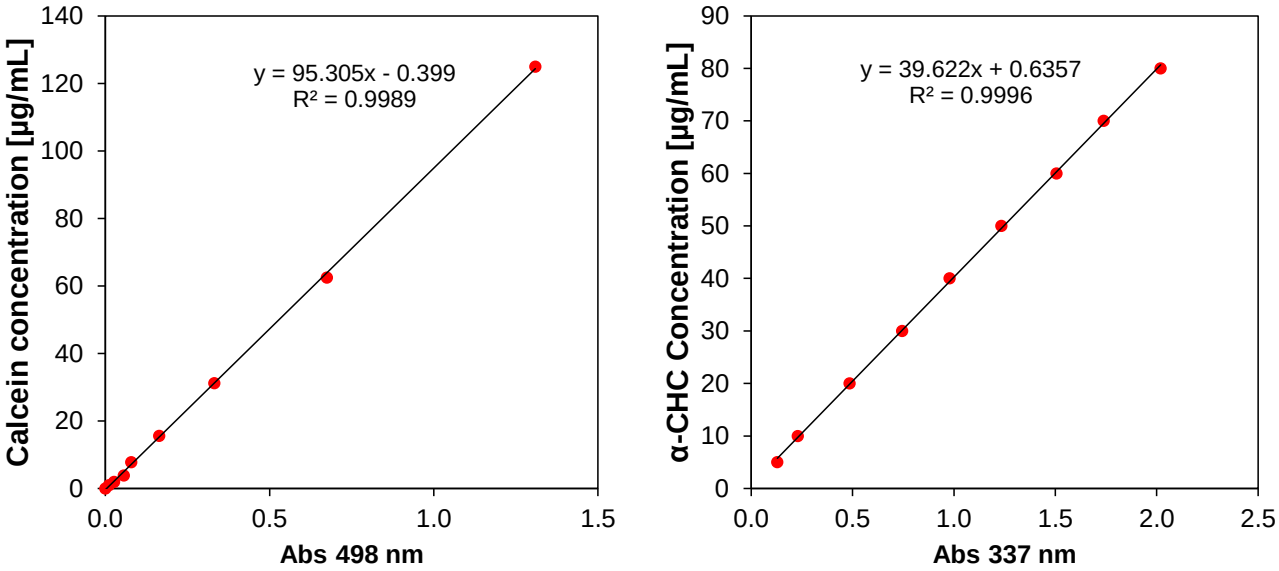

Figure S15. Calibration curve in PBS pH 7.4 for calcein (left) and α-CHC (right) used for the release experiments.